Scattering Model for Electrical-Large Target Employing MLFMA and Radar Imaging Formation

Xia Wu · Yaqiu Jin

Abstract

To numerically calculate electromagnetic scattering from the electrical-large three-dimensional(3D) objects, the high-frequency approaches have been usually applied, but the accuracy and feasibility of these geometrical and physical optics(GO-PO) approaches, to some extent, are remained to be improved. In this paper, a new framework is developed for calculation of the near-field scattering field of an electrical-large 3D target by using a multilevel fast multipole algorithm(MLFMA) and generation of radar images by using a fast back-projection(FBP) algorithm. The MPI(Message Passing Interface) parallel computing is carried out to multiply the calculation efficiency greatly. Finally, a simple example of perfectly electrical conducting(PEC) patch and a canonical case of Fighting Falcon F-16 are presented.

Key words : Numerical Calculation, Scattering, Target, MLFMA.

Ⅰ. Introduction

Nowadays, various kinds of radars are widely employed in mapping and surveying as a versatile remote sensing instrument[1]. Whether the satellite remote sensing or synthetic aperture radar(SAR), the image formation is based on the scattering mechanism of the observation target. The scattering computation for complex objects played an important role. For a long time, because targets with electrically large scales have highly involved and complex surfaces and features, numerical methods are limited due to the huge increase in computation consumption.

On the other hand, it is commonly believed that electrically large targets are in the optical region, several high-frequency approaches, such as the geometrical and physical optics(GO and PO) approaches, and ray tracing method, have been usually applied[2],[3]. However, the accuracy and feasibility of these GO-PO approaches are remained to be improved.

In this work, we calculated the scattering of the electromagnetic wave from electrical-large targets by using a multilevel fast multipole algorithm(MLFMA)[4].

The MPI(Message Passing Interface) parallel computing was carried out to multiply the calculation efficiency greatly[5]. Furthermore, we analyzed the task of generating radar images from the scattering field results. A fast back-projection(FBP) algorithm was utilized for image reconstruction motivated by its accuracy and less computational cost[6].

The remainder of this paper is organized as follows. In the next section, we give a short overview of the system flow and the formulations of MLFMA, and FBP is briefly described. Section Ⅲ is numerical study which discussed the quality of the generated radar image. Section Ⅳ concludes this paper.

Ⅱ. Formulation and System Flow

2-1 System Flow

The procedures of the entire system are divided into four parts: the preprocessing, the electromagnetic simulation process, fast computing, and the post-processing. The flow chart was illustrated in Fig. 1.

Fig. 2 presents the top view of the mesh generation by Gmsh[7] from a canonical Fighting Falcon F-16.

2-2 MLFMA Formulation

The MLFMA is referred to in several papers[4],[8]. Hereby, a combined-field formulation that includes the electric-field integral equation(EFIE) and the magnetic-field integral equation(MFIE) is employed for conducting targets:

$$CFIE = \alpha\, EFIE + (1-\alpha)\, MFIE \qquad \alpha = 0.2 \sim 0.8 \tag{1}$$

in which, $EFIE$: $n \times L(\bar{J}_s) = n \times E^{inc}$ (2)

$$MFIE:\ \frac{1}{2}\bar{J}_s(r) + n \times \tilde{K}(\bar{J}_s) = n \times \bar{H}^{inc} \tag{3}$$

Manuscript received April 14, 2010 ; revised August 30, 2010. (ID No. 20100414-14J)

Key Laboratory of Wave Scattering and Remote Sensing Information (Ministry of Education), Fudan University, Shanghai, P. R. China.
Corresponding Author : Xia Wu (e-mail : wuxiaeecs00@gmail.com)

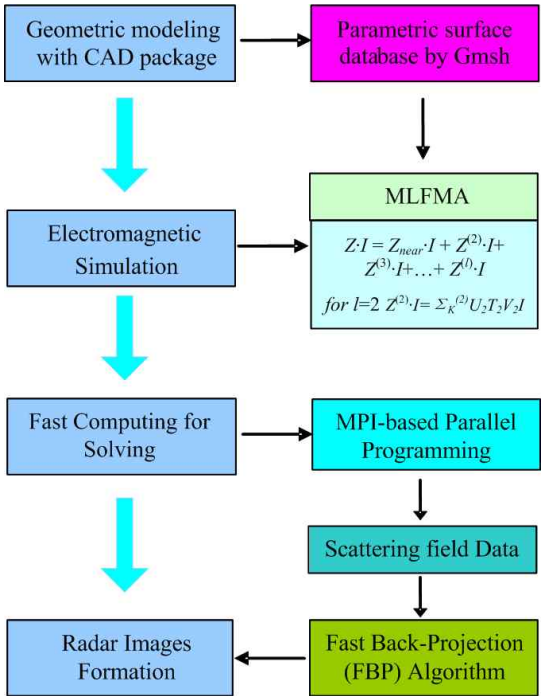

Fig. 1. Flow of EM simulation and radar images formation.

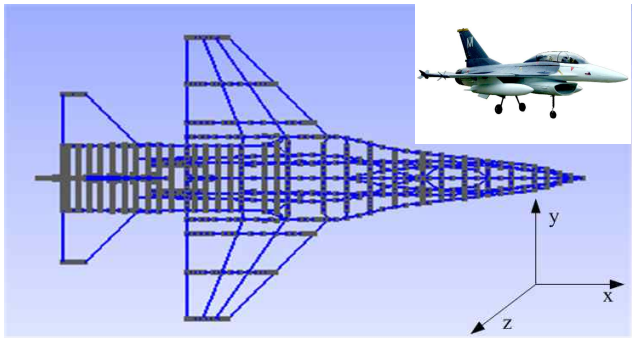

Fig. 2. 3D mesh of F-l6 generated by Gmsh.

where $\bar{J}_s = \eta J_s$, $\bar{H}^{inc} = \eta H^{inc}$, $\bar{J}_s$ is the equivalent surface current and η is the wave impedance, respectively. Vector integral operator L and K are defined as follows:

$$L(X) = jk_o \iint_s \left[X(r') G(r,r') + \frac{1}{k_0^2} \nabla' \cdot X(r') \nabla G(r,r') \right] dS' \tag{4}$$

$$K(X) = \iint_s X(r') \times \nabla G(r,r') dS' \tag{5}$$

G represents Green function in 3D free space, $\tilde{K}$ is the principal value integral of K.

The impedance matrix in MLFMA can be expressed as:

$$Z = Z_{near} + \sum_{i=2}^{l} Z^{(i)} \tag{6}$$

where Z_{near} includes the interaction matrix in neighbor cubes, $Z^{(i)}$ denotes the ith level interaction matrix in far cubes. For instance, while l=3,

$$Z^{(3)} = \sum_{K^{(3)}} U_3 T_3 V_3, \quad Z^{(2)} = \sum_{K^{(2)}} U_3 W_{2\to3} T_2 W_{3\to2} V_3 \tag{7}$$

in which, $[U]$, $[T]$, $[V]$ are depolymerization matrix, transfer matrix, and aggregation matrix, respectively. $W_{i\to j}$ represents the interpolation matrix(if $i>j$) or otherwise anti-interpolation matrix(if $i<j$). A Lagrange interpolation method is used for the interpolation calculation between levels[9].

2-3 FBP Algorithm

The emergence of back-projection(BP) method was in tomography based on FFT. Then a fast back-projection algorithm was proposed to reconstruct a radar image[10].

The radar imaging model was sketched in Fig. 3. The transmitter was fixed at 60º elevation and 90º azimuth, and the distance between the receivers and origin of coordinates is chosen to be 100 m.

For a given transmitter position, and given frequency and polarization of transmission, we defined (x_t, y_t) as the transmitter position point and (x_r, y_c) as the receiver position point. The distance from the receiver to a scattering point at (x, y), which is an arbitrary point unit of the targets, can be written as

$$R = \sqrt{(x_r - x)^2 + (y_c - y)^2} \tag{8}$$

The radar echo at each location of receivers is numerically calculated by the MLFMA-MPI EM simulation process. The return signal can be regard as the integral of all the point unit shown as follows

$$d(x_r, \omega) = \iint g(x,y) \exp(-j\omega R / c) dx dy \tag{9}$$

Back-projection reconstructs the image by back-projecting the projections along the original paths of integration[11], and yields

$$g(x,y) = \sum_{h=1}^{N_h} \int d(x_{rh}, \omega) \exp(-j\omega R_h / c) d\omega \, \Delta x_{rh} \tag{10}$$

where N_h is the number of the locations, R_h is the range between the h-th antenna and scattering point, with

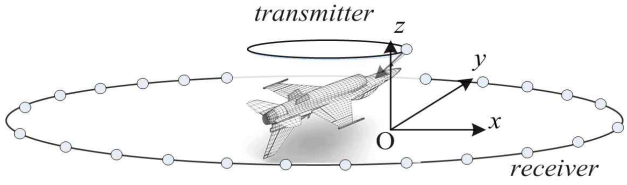

Fig. 3. Radar image mode scenario.

delay Δx_{rh}.

For an $N\times N$ image, traditional back-projection has $O(N^3)$ complexity, while a fast back-projection has $O(N^2\log_2 N)$ complexity. The main idea of this fast algorithm can be regard as the superposition process of sub-images and forming new beams. Moreover, in the near-field scenario, wavefront curvature cannot be neglected, thus traditional back-projection is not suitable in the near-field scenario. The proposed fast back-projection avoids frequency-domain interpolation, which can be modified for the near-field scenario[6].

Ⅲ. Numerical Results

The first simple example is a square perfectly electrical conducting(PEC) patch of 0.5×0.5 m size. The center of patch is located on $(1.5\hat{x},\ -2.4\hat{y},\ 0\hat{z})m$. The incident field is a plane wave propagating in the positive y direction, and the receivers distributed in an arc around the negative y direction on the xy plane, and the imaging is also done in the xy plane. Table 1 illustrates the range resolution in this work for a given bandwidth (BW).

In this case, the bandwidths were chosen to be 200 MHz and 500 MHz, respectively, and the numbers of receiver azimuth angles are correspondingly 64 and 257. EM simulation gives the scattering field data in both H and V polarizations of the receiver for the above parameters. For transmitting and receiving horizontal polarization(HH) in radar systems, the scattering results are imaged in Fig. 4. Its profile can be detected clearly when BW is equal to 500 MHz.

The second case is the F-16 whose geometric model is shown in Fig. 2. The incident field propagates along the direction with a 60º angle towards positive y direction(sketch in Fig. 3). With receiver position varying over the azimuth angle φ_s through 0º to 360º, each run gives the data collected for a certain range of receiver angles for the bandwidth of frequencies. The scattered field in both H and V polarizations were plotted in Fig. 5 and HH, HV, VH and VV polarization images were

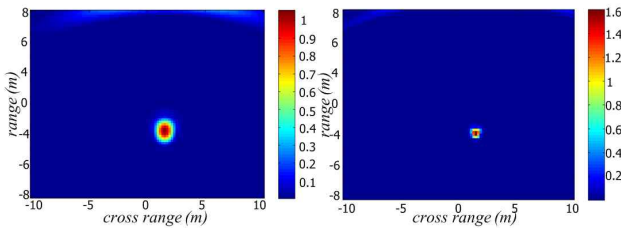

Fig. 4. Radar image of the patch BW=200 MHz vs 500 MHz.

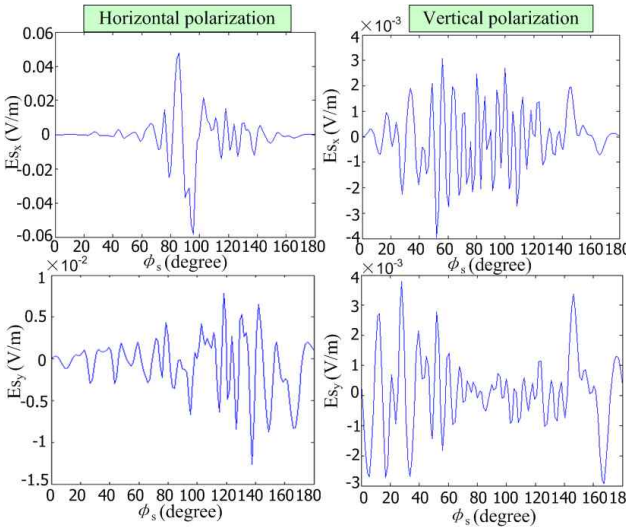

Fig. 5. Simulation scattering results at frequency=500 MHz.

shown in Fig. 6, respectively. Hereby, Kaiser window function for filter with a fixed parameter(β=2.2) was required to suppress unnecessary sidelobe contribution[12].

All the computation is carried on a master node of a parallel cluster, with configuration of 2.0 GHz CPU, 8 GB total memory and 2 Intel quad core. Table 2 illustrates the RWG numbers, total size of Z_{near} matrix and

Table 1. Range resolution for given bandwidth(BW).

BW (MHz)	Low freq. (MHz)	High freq. (MHz)	Sweep frequencies	Range resolution
200	200	400	16	0.75 m
500	500	1,000	40	0.30 m

Table 2. Comparison of RWG numbers, total size of Z_{near} matrix and run time vs frequency.

Numerical case	Freq. (MHz)	Number of RWG	Total size of Z_{near} matrix (MB)	Run time (second) (8 CPU)
Square	200	36	0.01	0.8
	400	144	0.09	1.6
	500	260	0.24	2.89
	1,000	944	1.2	4.72
F-16	200	20,701	53.6	138.05
	400	84,153	221.5	584.89
	500	132,631	352.5	1,123.05
	666.7	236,298	615.0	2,501.02
	1,000	538,532	1,338	4,596.11

Table 3. Comparison of time cost with MPI-based parallel program.

BW (MHz)	Sweep frequencies	Run time for complete MLFMA solution		
		2 CPU	8 CPU	128 CPU
200	16	5.2 h	96.2 min	12.2 min
500	40	204 h	63.6 h	-

run time for the bandwidth of frequencies with two numerical cases. The total run time was mostly dependent on MLFMA iterations and solution. According to the practice, iteration numbers were independent on the frequency increase. Table 3 gives the time required for computation under various hardware configurations and shows the efficiency of MPI-based parallel program.

Obviously seen from Fig. 5 and Fig. 6, the intensity of HH and VV images are stronger than those of HV and VH ones. Moreover, the vertical tail and the nose

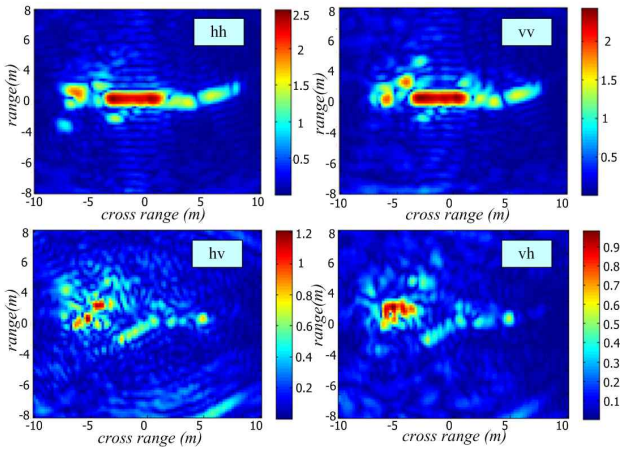

(a) BW=200 MHz

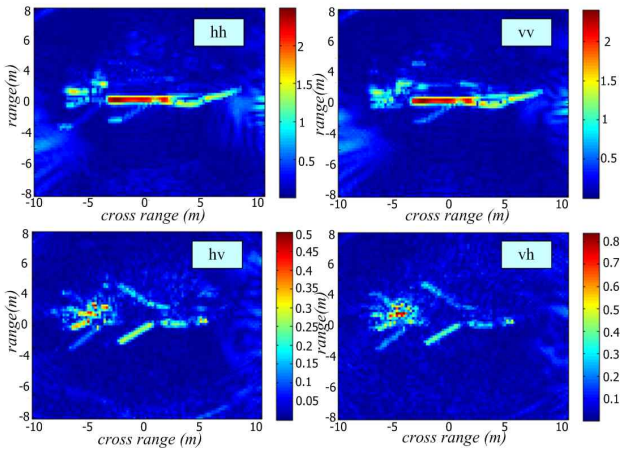

(b) BW=500 MHz

Fig. 6. Radar image of the F16.

can be clearly seen in HH and VV images, while the wings almost disappeared. This is because the specular reflection from the fuselage is quite powerful, which causes the coverage of the relatively weak edge diffraction from the wings. In case of HV and VH images, the vertical tail can be detected, and a vague outline of the wings is now visible. With 500 MHz bandwidth, higher range resolution is obtained than those with 200 MHz bandwidth. Consequently, the final results are of acceptable quality.

Ⅳ. Conclusion

This paper presented the near-field scattering field calculation by employing MLFMA with MPI parallelization. In addition, a fast back-projection(FBP) algorithm was applied to radar images formation. Two numerical examples were presented to verify that the achieved imaging results are of acceptable quality. Although the exact position of the scattering centers could not be calculated, the generated radar images are accurate.

References

[1] F. Xu, Y. Q. Jin, "Imaging simulation of bistatic synthetic aperture radar and its polarimetric analysis", *IEEE Trans. Geosci. Remote Sens.*, vol. 46, no. 8, pp. 2233-2248, Aug. 2008.

[2] R. S. Longhurst, *Geometrical and Physical Optics*, 3rd Ed., London: Longman, 1973.

[3] G. A. Deschamps, "Ray techniques in electromagnetics", *Proc. IEEE*, vol. 60, no. 9, pp. 1022-1035, Sep. 1972.

[4] J. Song, C. C. Lu, and W. C. Chew, "Multilevel fast multipole algorithm for electromagnetic scattering by large complex objects", *IEEE Trans. Antennas Propagat.*, vol. 45, no. 10, pp. 1488-1493, Oct. 1997.

[5] W. Gropp, E. Lusk, and A. Skjellum, *Using MPI: Portable Parallel Programming with the Message Passing Interface*(*Scientific and Engineering Computation*), 2nd Ed., the MIT Press, Nov. 1999.

[6] S. Xiao, D. C. Munson, S. Basu, and Y. Bresler, "An N^2logN back-projection algorithm for SAR image formation", *the Thirty-Fourth Asilomar Conference on Signals, Systems and Computers, Pacific Grove*, CA, USA, vol. 1, pp. 3-7, Oct. 2000.

[7] C. Geuzaine, J. F. Remacle, "Gmsh: A 3-D finite element mesh generator with built-in pre- and post-processing facilities", *Int. J. Numer. Meth. Engng.*, vol. 79, pp. 1309-1331, 2009.

[8] X. Q. Sheng, J. M. Jin, J. M. Song, W. C. Chew,

and C. C. Lu, "Solution of combinded-field integral equation using multi-level fast multipole algorithm for scattering by homogeneous bodies", *Annu. Rev. Progr. Appl. Comput Electromagn*., vol. 1, pp. 397-404, Mar. 1998.

[9] E. Castillo, A. Cobo, J. M. Guti´errez, and R. E. Pruneda, *Functional Networks with Applications: A Neural-Based Paradigm*, Kluwer Academic Publishers, 1999.

[10] S. Basu, Y. Bresler, "$O(N_2 \log_2 N)$ filtered backprojection reconstruction algorithm for tomography", *IEEE Trans. Image Processing*, vol. 9, no. 10, pp. 1760-1773, Oct. 2000.

[11] Y. Ding, Jr. D. C. Munson, "A fast back-projection algorithm for bistatic SAR imaging", *Proceedings 2002 International Conference on Image Processing*, vol. 2, pp. 449-452, Sep. 2002.

[12] J. F. Kaiser, "Nonrecursive digital filter design using the I_0 - sinh window function", *IEEE Int. Symp. on Circuits and Syst.*, San Francisco, CA, USA, pp. 20-23, Apr. 1974.

Xia Wu

received the B.S. and Ph.D. degrees from Peking University, Beijing, China, in 2004 and 2009, respectively. Her main research interests include electromagnetic scattering modeling, and computational electromagnetics.

Yaqiu Jin

received the B.S. degree from Peking University, Beijing, China in 1970, and the M.S., E.E., and Ph.D. degrees from the Massachusetts Institute of Technology, Cambridge, in 1982, 1983, and 1985, respectively. He is currently a Professor with the School of Information Science and Engineering, Fudan University, Shanghai, China.His main research interests include scattering and radiative transfer in complex natural media, microwave remote sensing, as well as theoretical modeling, information retrieval and applications in atmosphere, ocean, and Earth surfaces, and computational electromagnetics.